# Supporting Information

## Photoferroelectric Coupling and Polarization-Controlled Interfacial Band Modulation in van der Waal Compound $CuInP_2S_6$

Subhashree Chatterjee, Rabindra Basnet, Rajeev Nepal, and Ramesh C. Budhani*

*Department of Physics, Morgan State University, Baltimore, MD, 21251, USA*

*ramesh.budhani@morgan.edu

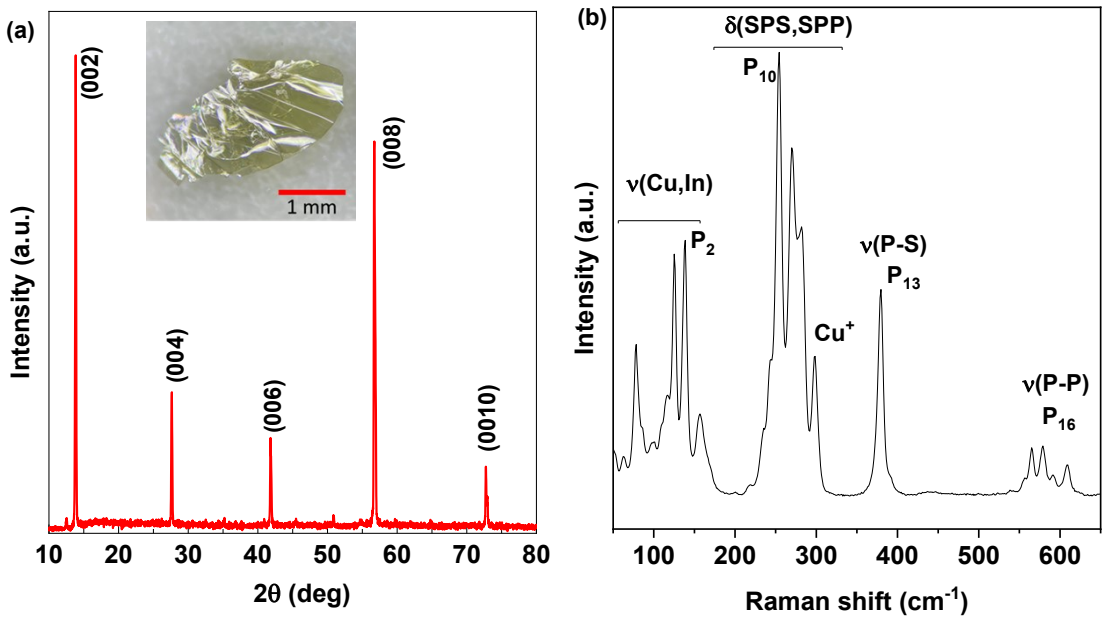


Fig. S1: Room temperature X-ray diffraction pattern, shown in Fig. S1a, confirms the structural quality and orientation of the as-grown crystals. Only (*00L*) reflections appeared, such that the scattering vector was parallel to the c-axis, indicating surface orientation normal to the c-axis. The as-growth, millimeter-sized, green, plate-like single crystals with flat, transparent surfaces are shown in the inset to Fig. S1a. The phase purity of CIPS is also confirmed from the Raman spectroscopy measurement of the as-grown crystal, as shown in Fig. S1b. All the vibrational modes are consistent with the previously reported data.[1]

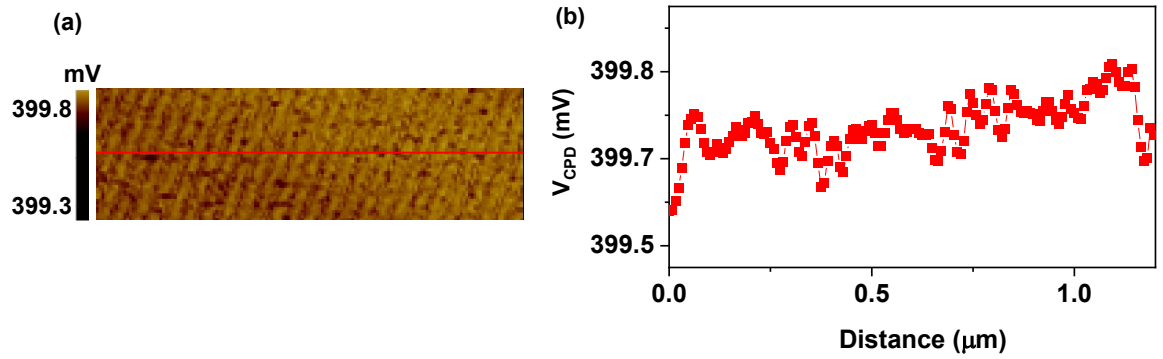


Fig. S2: KPFM $\phi_w$ measurement of Au-coated tip using standard HOPG sample. (a) KPFM surface potential ($V_{CPD}$) of the HOPG sample measured using an Au-coated tip. (b) $V_{CPD}$ line profile measured across the red line shown in (a). $\phi_{w\text{-}tip}$ of the Au tip is measured using the following formula:

$$\phi_{w\text{-}tip} = \phi_{w\text{-}HOPG} + eV_{CPD}$$

Where, HOPG work function, $\phi_{w\text{-}HOPG} \simeq 4.7$ eV, and $e$ is the electron charge

$V_{CPD} \simeq 0.399$ V

$\phi_{w\text{-}tip} \simeq 5.099$ V $\simeq 5.1$ eV

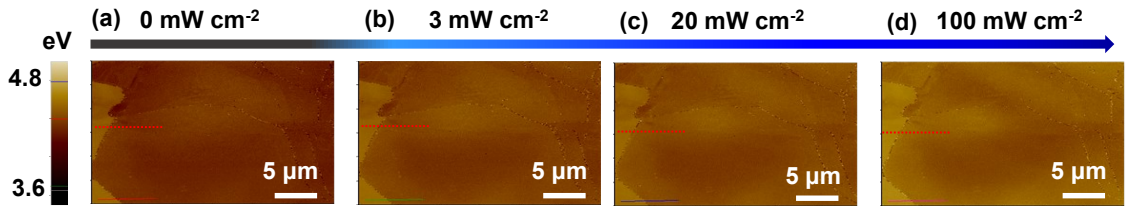


Fig. S3: KPFM $\phi_w$ of CIPS surface measured at different PD varying from 0-100 mW cm$^{-2}$: at (a) dark (0 mW cm$^{-2}$) , (b) 3 mW cm$^{-2}$, (c) 20 mW cm$^{-2}$, and (d) 100 mW cm$^{-2}$ illuminations. $\phi_w$ of CIPS is gradually increasing with increasing PD. The $\phi_w$ line profile is measured across the red dotted lines and plotted in Fig. 1d.

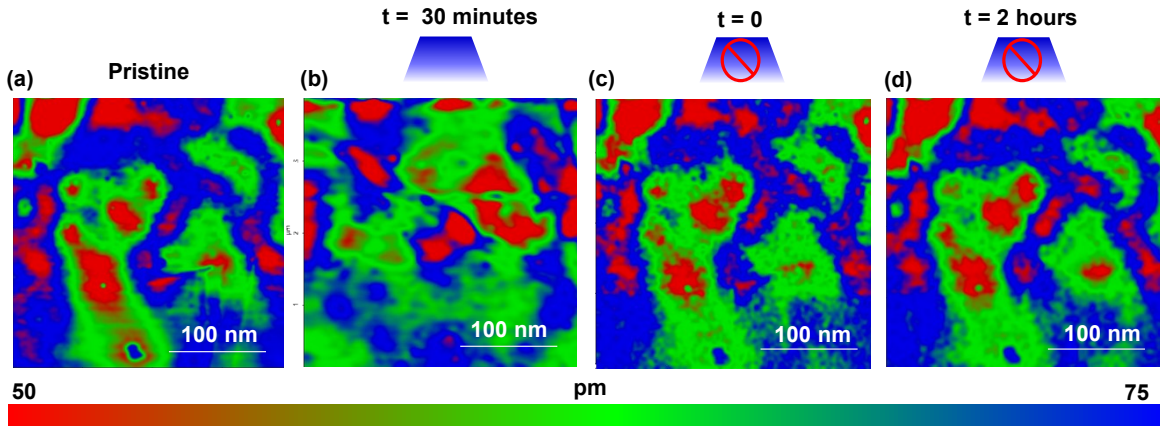


Fig. S4: Temporal evolution of the PFM amplitude images of a selected region of pristine CIPS flake before and after illumination. (d) Pristine CIPS, (e) 30 minutes after continuous light illumination, (f) immediately after the light is switched off, and (g) 2 hours after switching off the light. The PFM amplitude images show relatively smooth spatial variations rather than sharp minima at domain boundaries, likely due to contributions from substrate clamping, tip–sample contact stiffness, and electrostatic interactions influencing the measured electromechanical response.

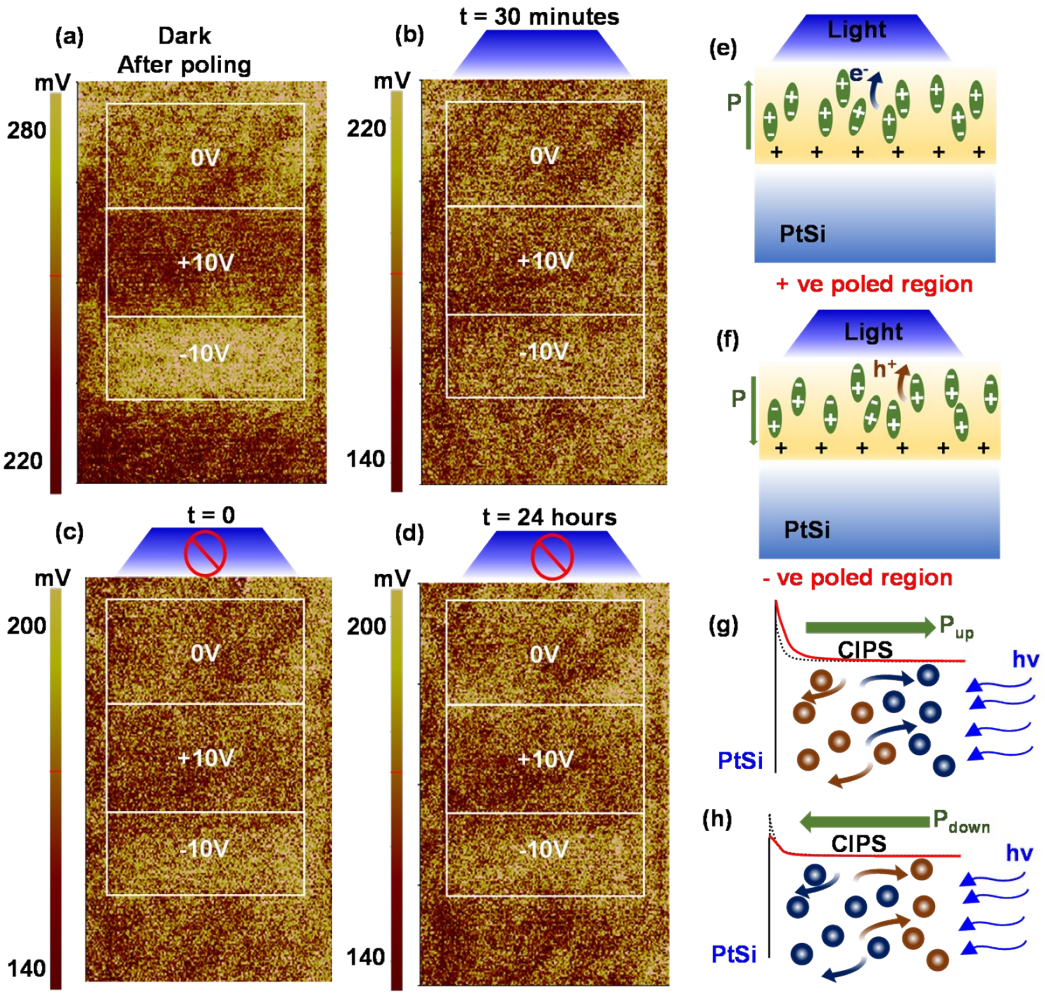


Fig. S5: Temporal evolution of the KPFM $V_{CPD}$ of a 50-nm-thick CIPS flake following local poling with a DC sample bias and subsequent illumination-driven relaxation. (a) $V_{CPD}$ image acquired immediately after poling without illumination, (b) after 30 minutes of continuous illumination in the same area, (c) $V_{CPD}$ measured immediately after the illumination is switched off, and (d) partial restoration of the potential contrast 24 hours after the illumination is removed. Under illumination, the photogenerated surface charge depends on the sign of the surface polarization-bound charge: electrons ($e^-$) accumulate in the positively poled regions (e), whereas holes ($h^+$) accumulate on the negatively poled regions (f). Here, the brown and blue arrows represent the direction of motion of photo-generated holes and electrons. (g,h) interfacial band bending diagrams and photogenerated carrier migration under illumination (hv) in different pre-poled states. Brown and blue circles represent the photogenerated hole and electrons, respectively.

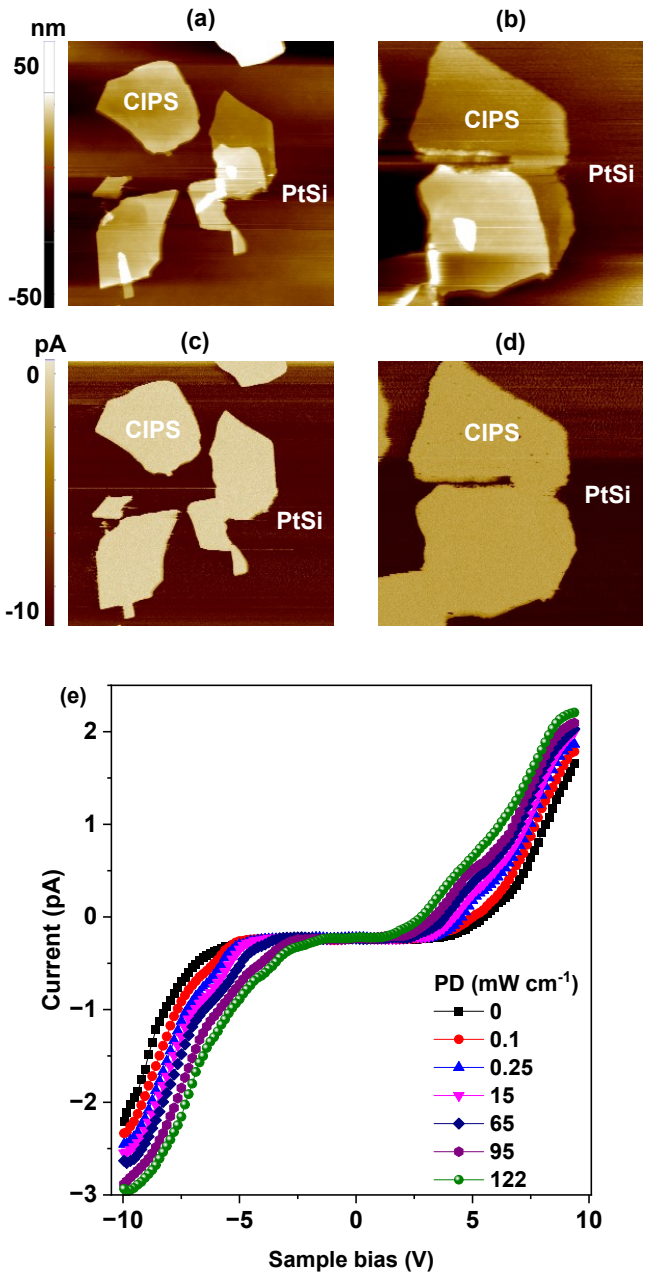


Fig. S6: C-AFM topography and current maps of CIPS layered flakes on a PtSi layer. (a,b) Topographic images of regions 1 and 2. (c,d) Corresponding current maps. (e) Room temperature *I-V* curves measured in C-AFM at different illumination conditions.

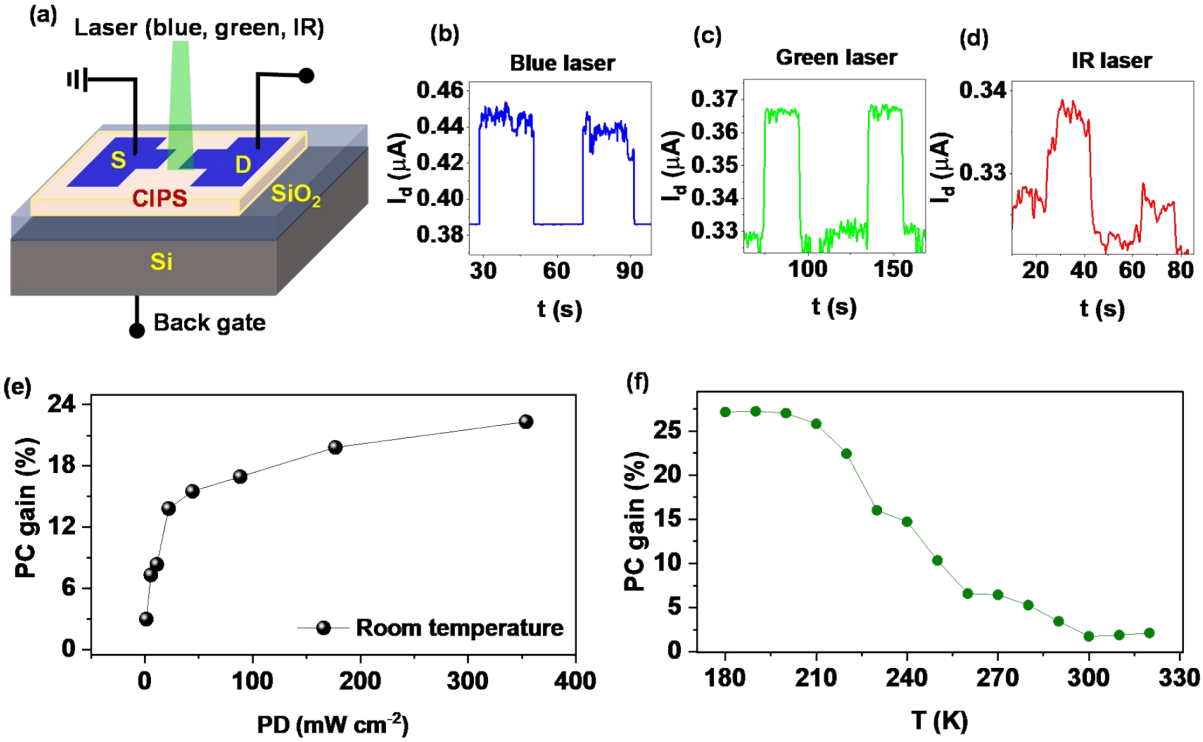


Fig. S7: Device schematic and electrical characterization of a CIPS-based field-effect transistor. (a) Schematic illustration of the CIPS channel device fabricated on a Si/$SiO_2$ substrate, showing the source (S) and drain (D) electrodes and back-gate configuration. (b–d) Representative drain current responses under light-on/off conditions, under blue, green, and infrared (IR) laser illumination. Photocurrent gain is maximum for the blue laser (445 nm). (e) Room temperature photocurrent gain at different illumination PD. (f) Temperature-dependent photocurrent gain from 180 K to 320 K. The gain increases with decreasing temperature.

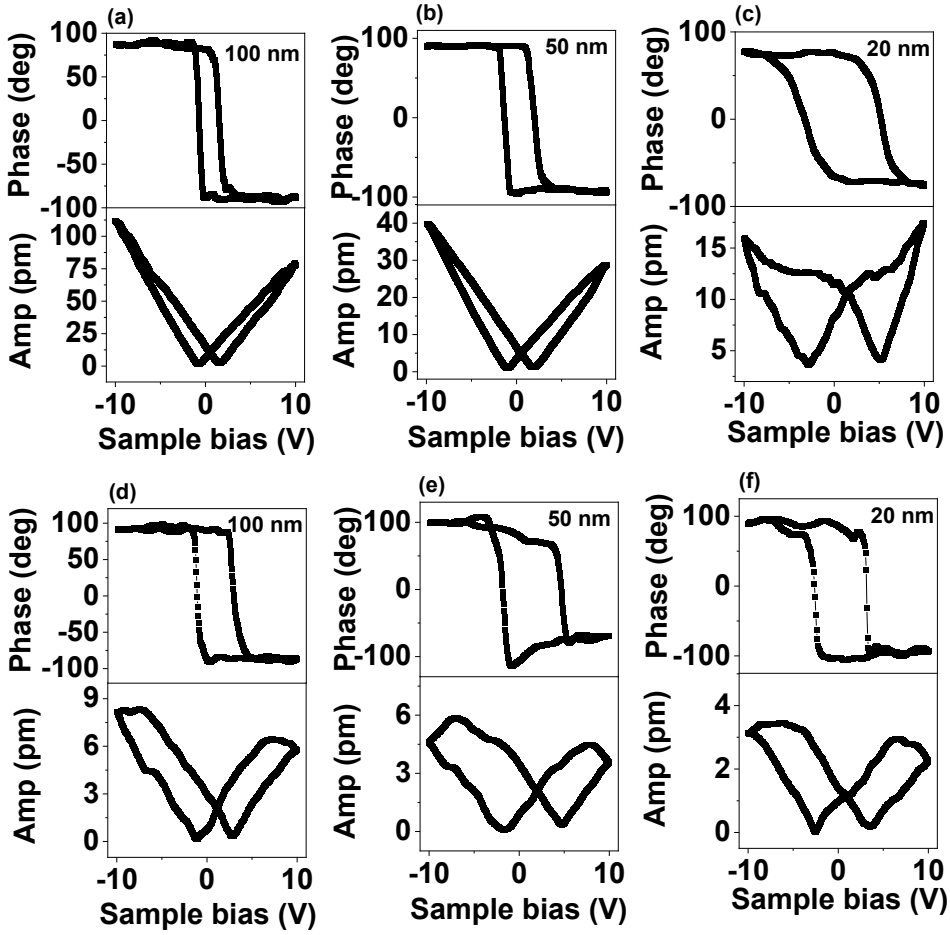


Fig. S8: Room-temperature FE and piezoelectric characterization of a layered CIPS flake by PFM. (a–c) Vertical PFM (VPFM) phase (upper panels) and amplitude (lower panels) hysteresis loops measured in off-state under ±10 V DC bias for CIPS flakes with thicknesses of 100 nm, 50 nm, and 20 nm, respectively. (d–f) Lateral PFM (LPFM) phase (upper panels) and amplitude (lower panels) hysteresis loops measured in off-state for CIPS layers with thicknesses of 100 nm, 50 nm, and 20 nm. The strong response observed in the VPFM measurements indicates a pronounced out-of-plane polarization in CIPS.

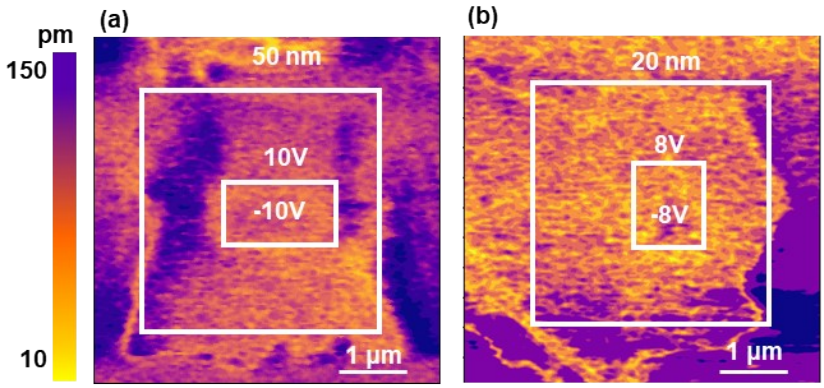


Fig. S9: (a, b) Vertical PFM (VPFM) amplitude image of a CIPS flake with 50 nm, and 20 nm thickness, respectively, after reverse DC bias poling.

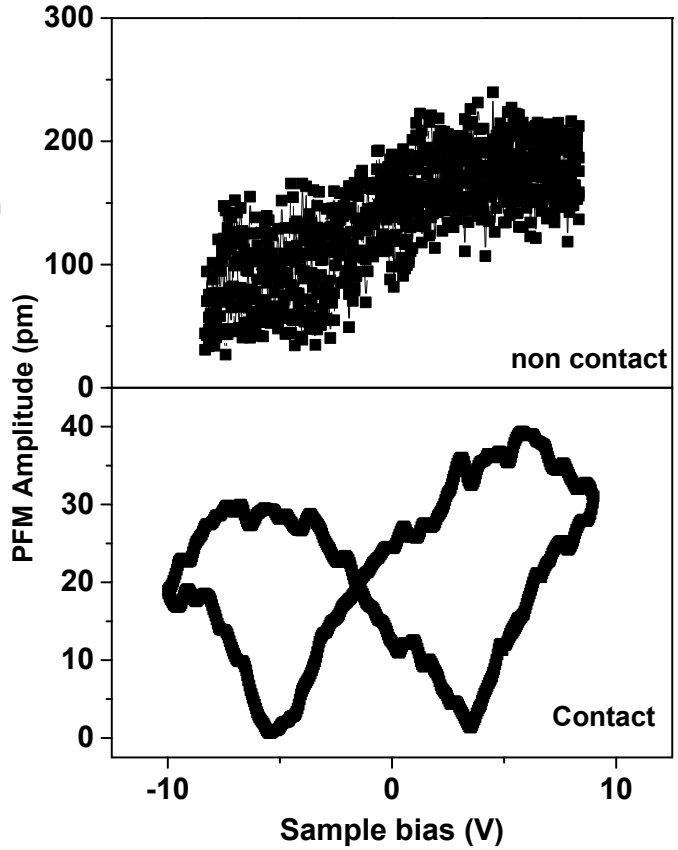


Fig. S10: PFM amplitude measured in a ~50 nm CIPS flake for non-contact (upper panel) and contact (lower panel) mode,[2] revealing true FE behavior in CIPS.

**References:**


1 R. Rao, B. S. Conner, J. Jiang, R. Pachter, M. A. Susner, *J. Chem. Phys.* 2023**, 159**, 224706.

2 S. Jesse, A. Belianinov, O. Ovchinnikov, S. V. Kalinin, *ACS Nano*, 2019, **13**, 8055–8066.